AT Technical memo series
AT/39.9/132

Accelerometer measurements on the Parkes Telescope

David McConnell, Brett Preisig

13 December 2012

Abstract

We have investigated the use of accelerometers to detect abnormal movements in the Base Tower of the Parkes Radio Telescope. The investigation was part of preparing a Telescope Protection System designed to allow safe, unattended operation of the telescope. Two accelerometers were fixed to the inside wall of the telescope tower and measurements were made during a variety of operations. We show that abnormal motions can be detected easily, and that the same accelerometer measurements may provide diagnostic information on the state of the telescope's mechanical systems.

Contents

1 Introduction

CSIRO intends to begin unattended operation of the Parkes rediotelescope in late 2012. Since the telescope's commissioning in 1961 it has the practice that its operator is located in the control room in the base tower. For some years now it has been technically feasible to control the telescope remotely, or automatically. However the telescope lacks the means of protecting itself against malfunction, and so it has become a policy that the operator should be located in the tower. To enable unattended operation, a protection system is being devised. This study of the telescope's vibrations is part of that development.

Section 2 describes the equipment and measurement process, and gives an analysis of the signal properties. Accelerometer data were collected on 20-22 June 2012. Over-night on 21 June normal astronomical observations were conducted. During business hours a number of operations were performed to provoke unusual, transient motions in the base tower. The transient responses and some analysis is given in §3, and in §4 we describe the accelerometer observations during normal telescope movements.

1.1 An early study

In 1966 the Division of Applied Physics was commissioned to conduct a vibration study of the telescope. The work was reported in a preprint [1], and subsequently published [2]. The main aims of the study were to experimentally determine the structural natural frequencies, and to observe the dynamic loading on the azimuth track associated with the vibrational modes and normal telescope operation. The report lists the measured vibration frequencies of major elements of the structure in response to various excitations.

2 Equipment and measurement

Two ICP® accelerometers (model 608A11[1]) were used, mounted radially and tangentially inside the outer wall of the tower, magnetically attached to a steel plate associated with the tower strengthening structure. The conditioned accelerometer signals were amplified using a pair of DC amplifiers with gain = 100 and time constant of 50ms. The amplified signals were sampled at 100Hz or 200Hz using a NI USB 6009 sampler, and recorded to disk. Figure 1 shows the experimental mounting of the accelerometers.

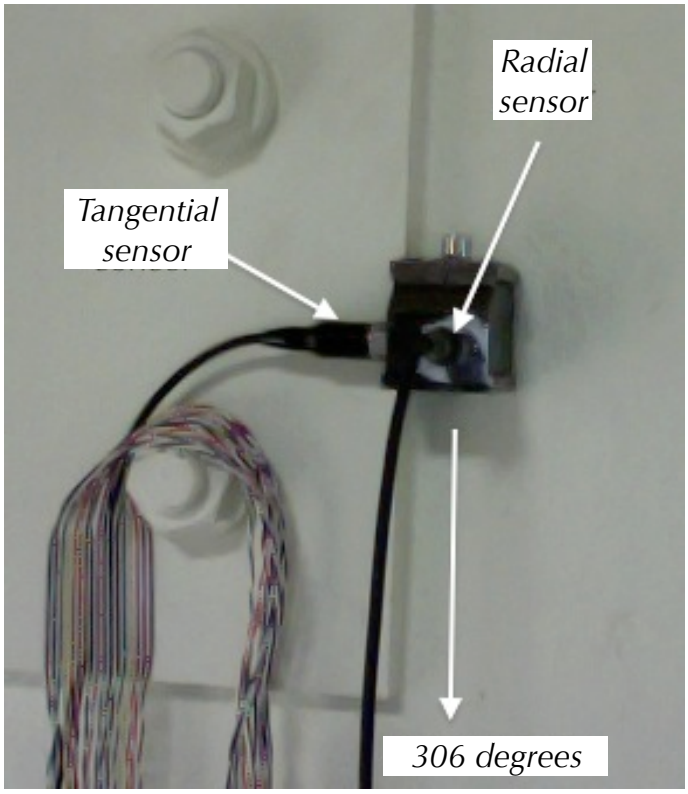

Figure 1: View of the trial accelerometer mounting inside the outer wall of the top level of the tower.

The accelerometer signal is handled as illustrated in Figure 2. The signal conditioner provides a constant current supply to the sensor, and presents its response as a voltage with a scale of 100 mV/g. In this experiment we amplified that voltage with a general purpose observatory amplifier with adjustable gain and output time-constant. The amplified signal was sampled

[1]ICP stands for "Integrated Circuit - Piezoelectric" and is a tradmark of PCB group, inc.

using a National Instruments NI USB 6009 unit. Data was collected from the sampler using NI Labview SignalExpress data-logging software.

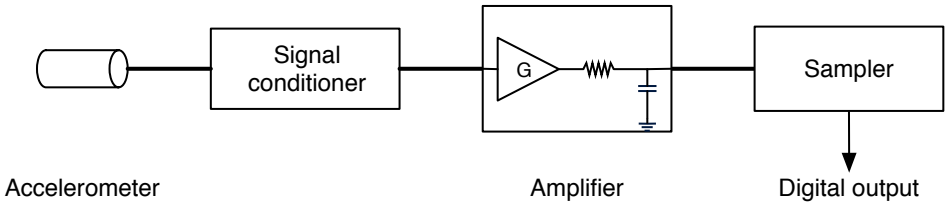

Figure 2: Signal path from accelerometer to computer. The amplifier was configured with gain $G = 100$ and time-constant $\tau = 50$ms.

2.1 The accelerometer signal

Figure 3 shows a sample of signal collected from a radially mounted accelerometer during routine telescope motion. The figure shows both the time-series data, and a power density spectrum. The data were taken with gain $G = 100$, time-constant $\tau = 50$ms, and a sampling frequency of 200Hz. We have modelled the spectrum as the sum of three components:

1. A low-level white component originating after the amplification stage, presumably associated with the sampler electronics. Little is known about this component, and its spectrum may not be white, but it probably extends far beyond the Nyquist frequency.

2. A "pink" or $1/f$ component associated with the amplifier itself.

3. The amplified accelerometer output. which is the sum of the accelerometer's internal device noise and its response to accelerations. The overall spectral shape of this component is determined by the low-frequency limit of the device response (0.5 Hz at -3dB) and the time-constant of $\tau = 50$ms chosen for the amplifier. The device noise ("Spectral noise" in the device specification sheet and in Table 1) has some frequency dependence. The dashed line in Figure 3 corresponds to that noise modified by the combined response of the amplifier and the device itself.

Some of the specifications of the 608A11 are reproduced in Table 1. The size of component 3 as shown in Figure 3 is estimated from the tabulated values of Spectral noise, converted to voltage using the nominal sensitivity. The size of the other components were adjusted to match their sum to the overall observed spectrum of the signal.

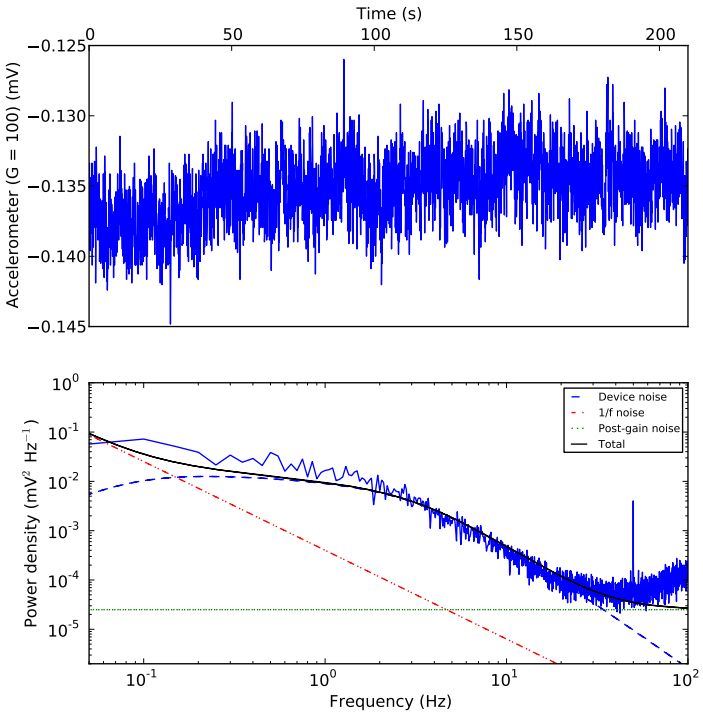

Figure 3: A sample of acceleration signal (top) and its power density spectrum (bottom). The shape of the spectrum can be understood in terms of three components: signal and internal noise from the accelerometer (labelled *Device*), $1/f$ noise, presumably from gain fluctuations on the amplifier, and noise added after the amplifier in the sampler and associated electronics, labelled *Post-gain noise*. The signature of a 50Hz contamination from the main power supply is clear, and there is evidence of aliased noise at the upper end of the spectrum.

3 Transient motions

Operators of the telescope occasionally report feeling motion in the base tower during periods of abnormal behaviour of the telescope controllers. Typically they report "rocking" or "swaying", and they may also report "creaking" noises. Items such as hanging cables are sometimes observed to swing during such events. To provoke motions such as these while recording accelerometer responses, we used the normal emergency stop mechanism (ESTOP) while the telescope was rotating in azimuth or elevation. The action of the ESTOP is to immediately remove all power from the drive motors and to apply brakes, which act on the shafts driven by each motor. Relative to the timescales of natural oscillation of the structure, the motor

Item	Value	
Sensitivity (±15%)	100	mV/g
Spectral noise (10Hz)	8	$\mu g/\sqrt{Hz}$
Spectral noise (100Hz)	5	$\mu g/\sqrt{Hz}$
Spectral noise (1kHz)	4	$\mu g/\sqrt{Hz}$

Table 1: Specifications of the ICP 608A11 accelerometer

shafts stop rotating instanteously. The telescope's response is expected to depend on its azimuth and elevation and its rotation rate at the time of the eSTOP, but as an eSTOP places stresses on the telescope's structure, we used this technique sparingly and so were unable to fully explore the range of responses. A similar technique for exciting transient vibrations was used by Macinante [1].

At an early stage of our investigations, using a single accelerometer mounted radially at $Az = 306\,^\circ$, the event shown in Figure 4 was recorded. In this case the eSTOP was activated with the telescope was at $(Az, ZA) = (110\,^\circ, 2\overset{\circ}{.}5)$, driving towards larger zenith angles at $12\,^\circ$/min. The tower motion in response to the sudden stop is clearly detected. In this case, the acceleration oscillates over a band of frequencies with a spectral peak at 2.75Hz and a maximum amplitude of 0.03 ms^{-2}. Direct integration of this record shows velocity and displacement peak amplitudes of about 0.0025 ms^{-1} and 0.0002 m (200μm) respectively.

With two perpendicular accelerometers (see Figure 1 we were able to verify that the direction of tower motion corresponds to expectations. Following Macinante et al. [2], define a coordinate system centered on the intersection of azimuth and elevation axes as illustrated in Figure 5 from [2]. With reference to this system, we expect oscillations in the YOZ plane to be excited by stopping drives about the OX axis, that is, stopping drives in zenith angle. We expect that stopping drives in azimuth (rotation about OZ) would excite torsional oscillations in the XOY plane. The two accelerometers were mounted horizontally (in the XOY plane) on the base tower wall perpendicular (referred to as "radial") and parallel (referred to as "tangential") to the wall. The tangential unit lies in the YOZ plane if the telescope's azimuth is set to $306\,^\circ$(or $180\,^\circ$away at $126\,^\circ$), whereas the radial accelerometer is parallel to that plane if the azimuth is set to $306\pm90\,^\circ$.

The records in Figure 6 show the response to excitations in the zenith angle direction with the telescope set to Azimuth $Az = 221\,^\circ$ (a) and $Az = 306\,^\circ$ (b). It can be seen that in panel (a) the radial accelerometer is close to being perpendicular to the YOZ plane and so registers little motion. Most of the motion is detected in the tangential accelerometer. In panel (b) the telescope's azimuth placed the elevation axis perpendicular to the

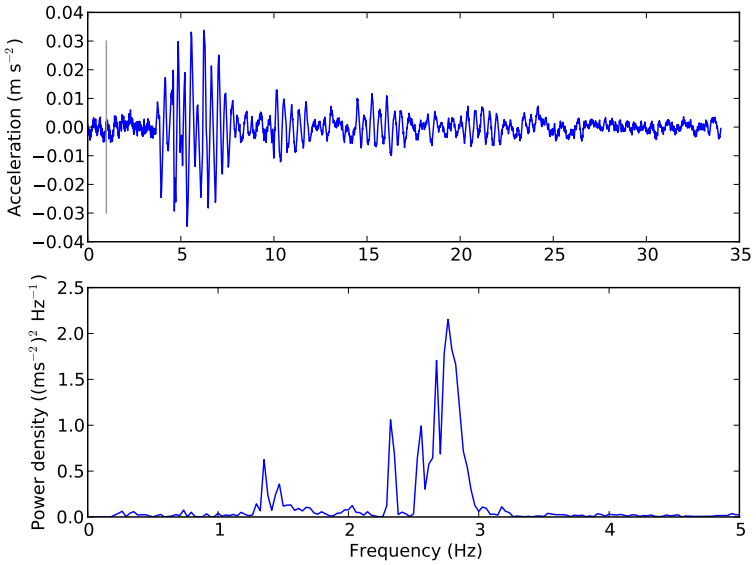

Figure 4: Accelerometer output during the recovery form an elevation ESTOP. The single accelerometer was mounted radially. The telescope's azimuth and elevation were 110 °and 2.5 °. The time of ESTOP activation is marked by a vertical line, several seconds before the onset of the strongest accelerations.

radial sensor, which now detects most of the motion. There is some evidence of detectable oscillations in the XOZ plane (radial sensor in panel (a) and tangential sensor in (b)). These correspond to the "lateral mode" described by Macinante.

In Figure 7 we show the results of an ESTOP activated while driving in azimuth. The dominant signal is detected in the tangential sensor, consistent with a torsional oscillation at a frequency of 1.07Hz. Macinante et al. reported a torsional mode of oscillation at 1.2Hz in response to the same kind of excitation. Their measurements were made at zenith angles of 0 °, 30 °and 60 °, and they reported less than 10% variation in the oscillation frequency.

Report on the following: 1. Base tower stiffening (1969) 2. Mass added to Focus cabin and counterweight (1996) 4. Reduce observations of transients to motion (displacement) of the sensor. 5. Demonstrate the directivity of the sensor arrangement.

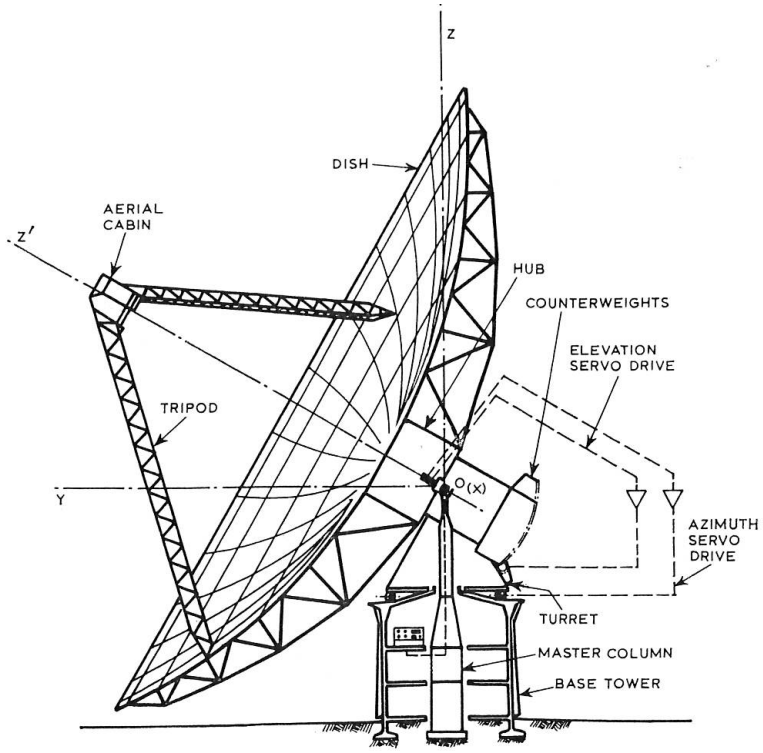

Figure 5: Nomenclature (Fig. 2., Macinante et al. [2])

4 Normal operation

Figures 1 and 2 are the spectrograms of the radially and tangentially mounted accelerometers. The upper plot of each shows the elevation of the telescope during the period of accelerometer measurements. There are four long periods (starting near 12h, 14.5h, 17h and 21h) when the telescope was wind stowed. During the first two of these it was actively held at a zenith angle of 1.6 ° by the drive motors. During the third and fourth, it was parked on the zenith stop with motors off. For most of the time while at low elevation (32 °) the telescope was taking data along long azimuth scans of speed about ±15 °/min.

What can be learned from them?

1. Electrical interference. It is possible that unwanted signals can enter the data between the sensor and the sampler (in either the constant-current signal conditioner or the DC amplifiers). Such interference would be have no dependence on telescope motion. Neither spectrogram shows any sign of such a signal, so we conclude that no significant unwanted signals enter from the electronics.

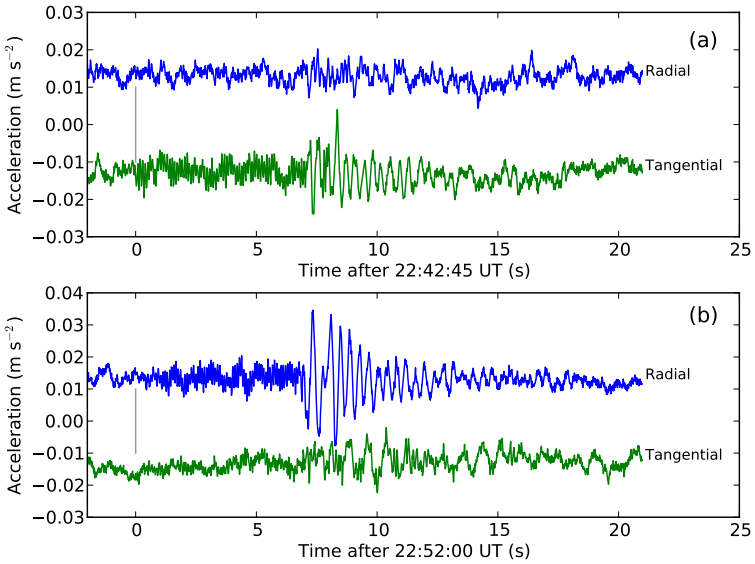

Figure 6: Dual accelerometer outputs during the recovery to elevation eStops. The telescope's azimuth was (a) 221 °and (b) 306 °. The time of each eStop activation is marked by a vertical line.

2. There is clear evidence of accelerations associated with telescope motion. Both spectrograms show a general increase in broadband noise when the telescope is moving. In addition there are many signals with discrete frequencies of bandwidth varying from the spectrograms' resolution (0.02Hz) to about 2 Hz (for example the sets of enhancements in Figure 2 in the time range 10h - 12h and near 12Hz and 47 Hz.

3. There are also discrete frequencies in the signal during the periods of no telescope motion. Figure 1 shows this near 12.6 Hz; figure 2 has several more pronounced bands between 8 and 18 Hz. In both figures, these bands fade between 18h and 20h. Figure 3 below shows the strength of the 12.6 Hz signal, and the wind speed. It seems plausible that wind above about 22 km/h (dotted line) drives a resonance in the telescope structure, but only when it is parked at the zenith.

4. Both spectrograms show strong broad-band noise while the telescope is slewing in zenith.

5. For extended periods the telescope was scanning in azimuth at a constant rate of 15 °/min. Knowing the details of the azimuth motion gearing allows tooth-frequencies to be calculated. There is no evidence of these frequencies in either spectrogram.

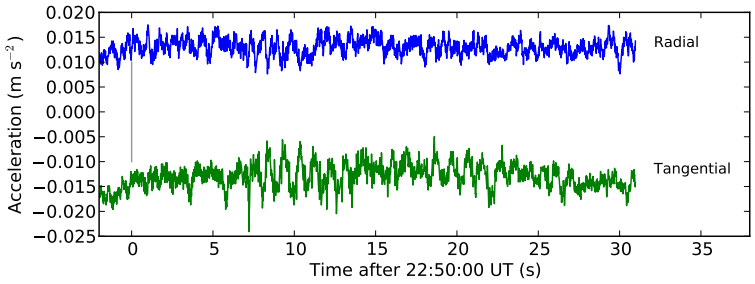

Figure 7: Dual accelerometer outputs during the recovery to an eStop activated while driving in azimuth.

6. Near 20h the tangential spectrogram shows detailed response to the set of short scans done at this time. Again, the observed signals do not correspond to any known motor speed or tooth frequency.

7. However, a signature of the zenith mechanism is seen during slews in elevation. Figure 4 below shows a portion of the spectrogram from the tangential accelerometer. A fine comb of frequencies are evident during all seven elevation slews. Figure 5 shows one of these. The comb spacing is df = 0.11976 Hz. The average zenith rate during this slew was 11.978 °/min. At this rate, the turning frequencies of the three spur gears are $f_3 = 0.01996$, $f_2 = 0.11978$ and $f_1 = 1.1978$ turns/second. The comb of frequencies indicates a brief pulse in the time domain with frequency equal to the comb spacing. That is equal to the rate of turn of the second spur gear, ie. $f_2 = df$. The second spur gear has 160 teeth, and we see a very strong signal at $160 \times f_2 = 19.161$ Hz (see Figure 6). The third spur gear has 96 teeth, and we see a signal also at $1.916 = 96 \times f_1$. No signal is visible at f_1, and its tooth frequency lies outside our frequency range. The f_2 signature suggests that the second spur gear delivers a sharp knock once per revolution. The presence of 100 harmonics indicates that the duration of the knock is no more than about 100th of a turn. Possible a single tooth on this gear in one of the Zenith gear boxes has an irregularity.

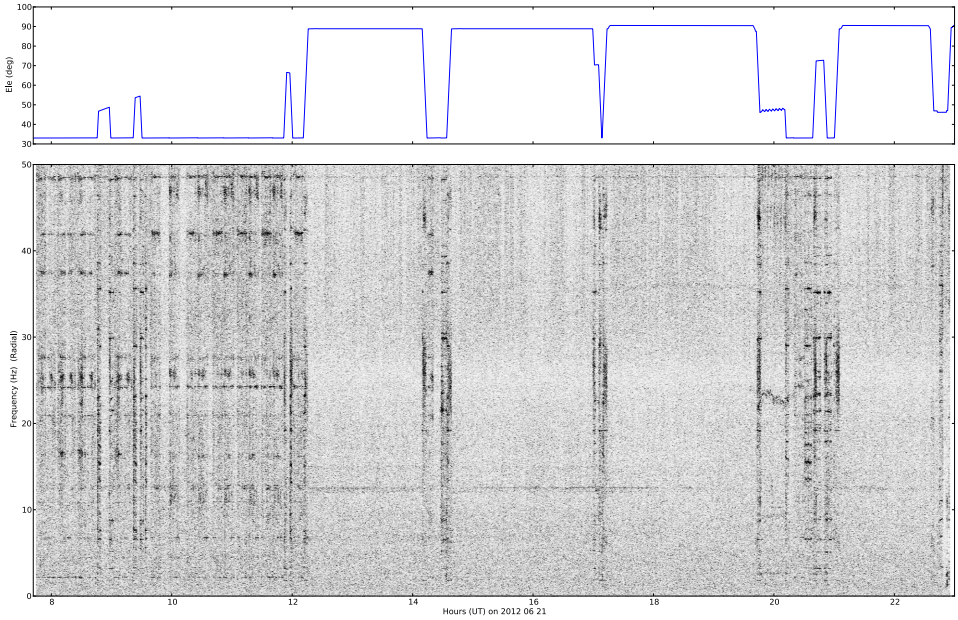

Figure 8: Spectrogram of the radial accelerometer signal.

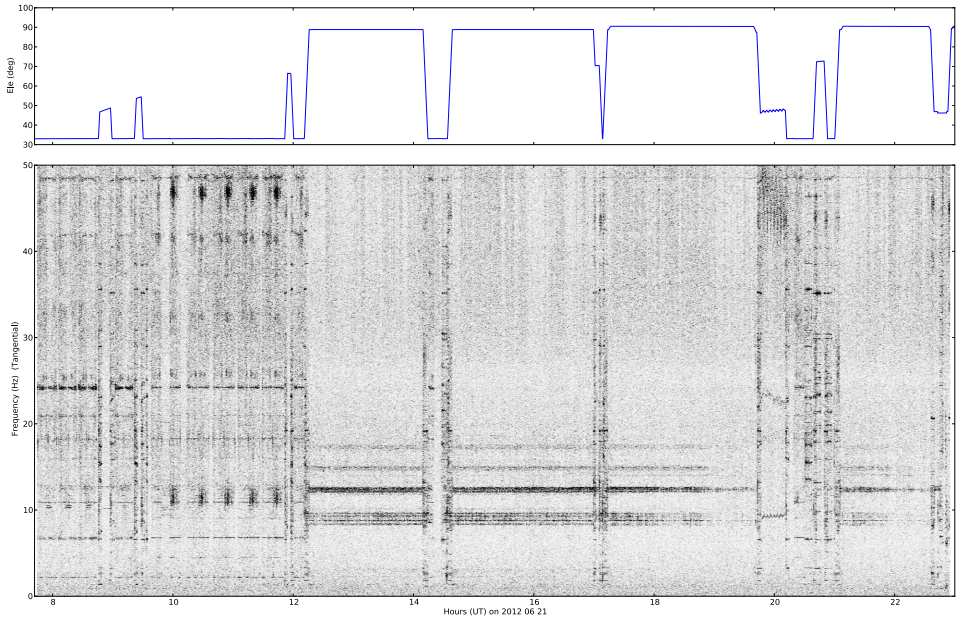

Figure 9: Spectrogram of the tangential accelerometer signal.

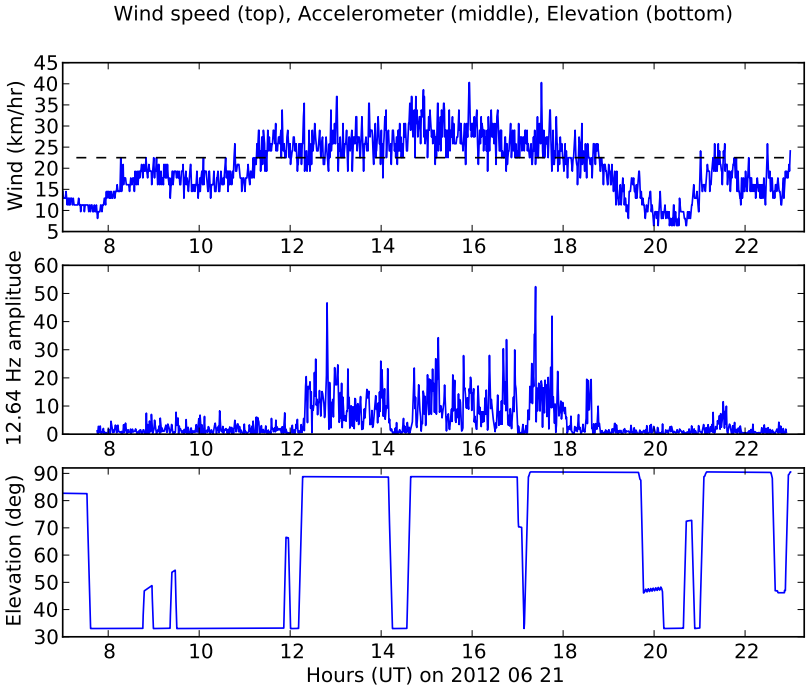

Figure 10: Wind speed, accelerometer output a(spectral component at 12.64Hz) and telescope elevation, showing the suggested resonance driven by the wind.

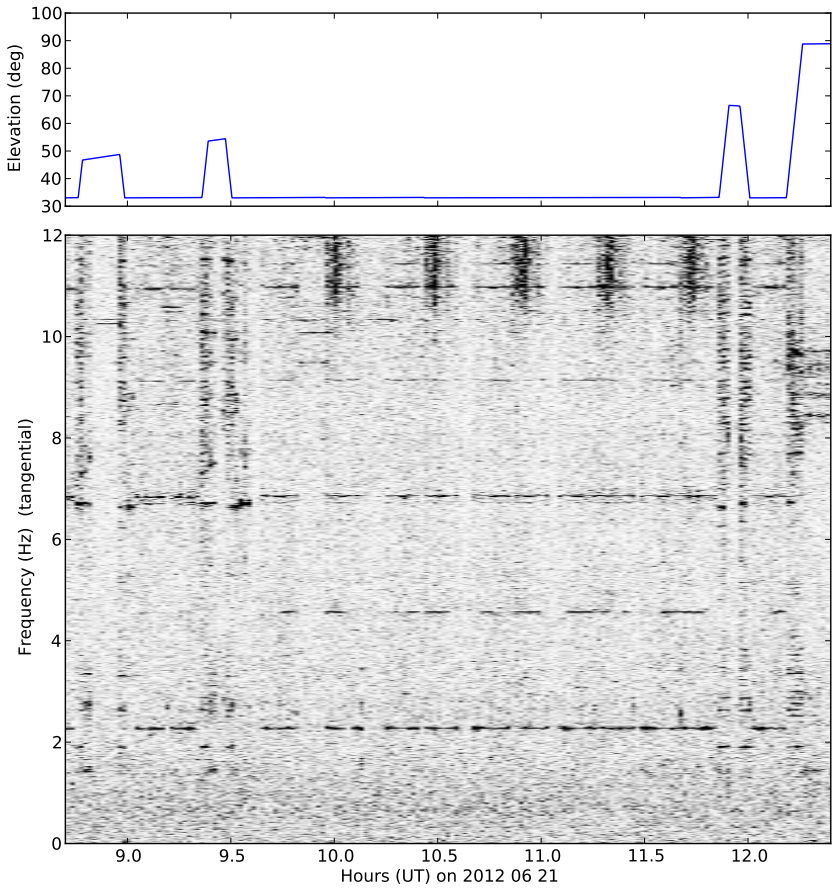

Figure 11: Spectrogram of the tangential accelerometer signal, showing the combs of frequencies during zenith slews.

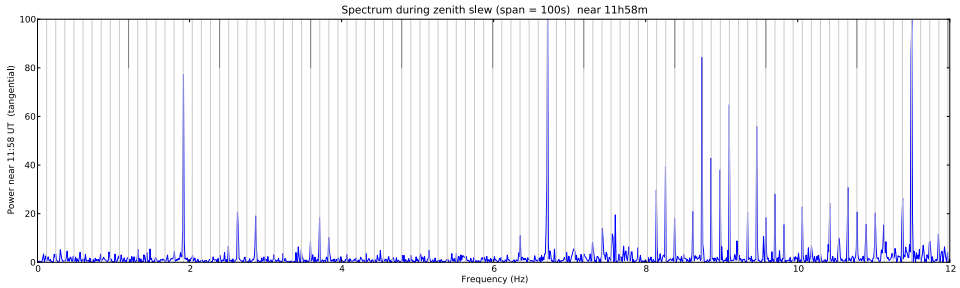

Figure 12: Tangential accelerometer spectrum during the zenith slew at 11:58 UT. This shows the comb of frequencies with spacing 0.1197 Hz. Multiples of this frequency are shown by vertical grey lines, every tenth is darker.

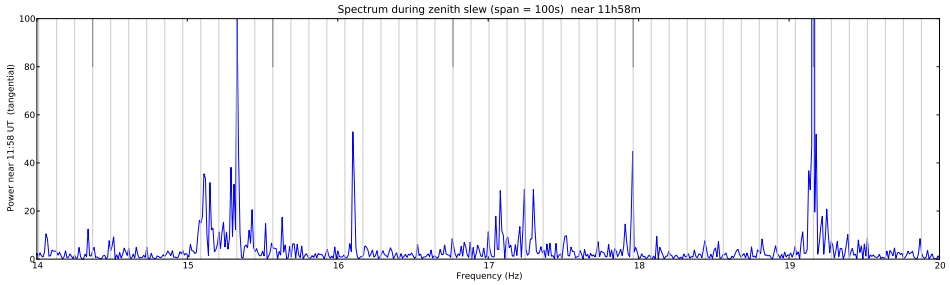

Figure 13: Tangential accelerometer spectrum during the zenith slew at 11:58 UT. This shows the strong component at $160 \times f_2 = 19.161$ Hz where f_2 is the turning rate (rev/second) of the stage II spur gear when driving in zenith at $11.98\,^\circ$/min. Multiples of the frequency comb spacing are shown by verticalgrey lines, every tenth is darker.

A Gear ratios and frequencies

The telescope is pointed at any part of the sky by rotation about the vertical axis (azimuthal motion) and about a horizontal axis (zenithal motion) mounted on the alidade. In each case a pair motors drive the telescope through gearboxes. The gear ratios and the numbers of teeth at each gearing stage need to be know to interpret periodic features observed in the accelerometer signals. Table 2 and the diagrams in Figure 14 summarise these quantities for each motion axis. Each stage in the gearing is characterised by a reduction ratio, normally given by the number of teeth the gear and on the pinion from the previous stage driving the gear. In the case of azimuth motion, the fourth stage reduction is mediated by the azimuth drive wheels (rollers) turning on the circular azimith track. The radii of these are 533.4mm and 5689.6mm respectively, giving the reduction ration shown in the table.

Table 2: Parkes Telescope motion gears. See text for an explanation.

Stage	Teeth		Reduction ratio		Cumulative ratio
	Gear	Pinion			
Azimuth					
Motor		19			
1	296	18	296:19	15.578947	15.578947
2	212	20	212:18	11.777778	183.48538
3	153		153:20	7.650000	1403.6632
4				10.666667	14972.407
Zenith					
Motor		17			
1	312	16	312:17	18.352941	18.352941
2	160	16	160:16	10.000000	183.52941
3	96	18	96:16	6.000000	1101.1765
4	648			36.000000	39642.353

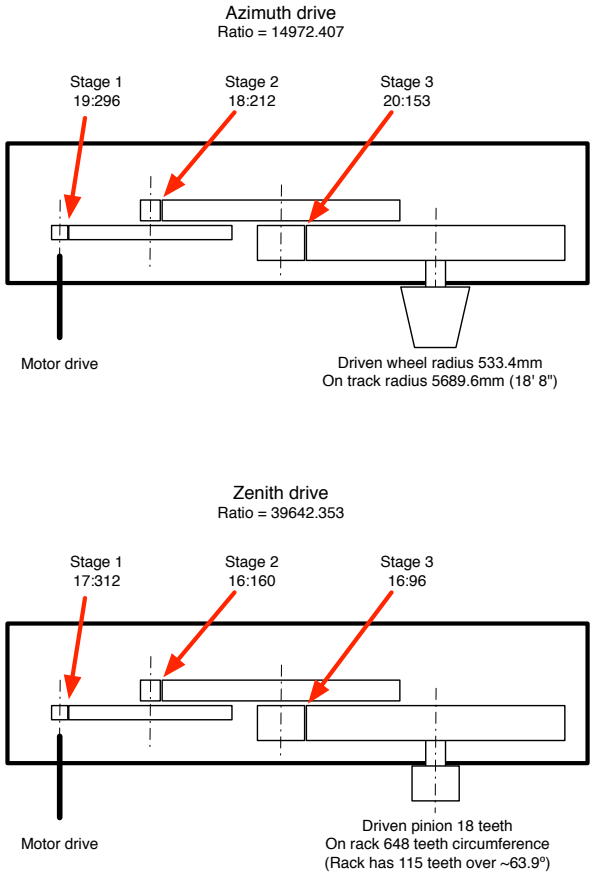

Figure 14: Diagrams of the arrangement of gears in the azimuth and elevation drives of the Parkes 64m telescope.

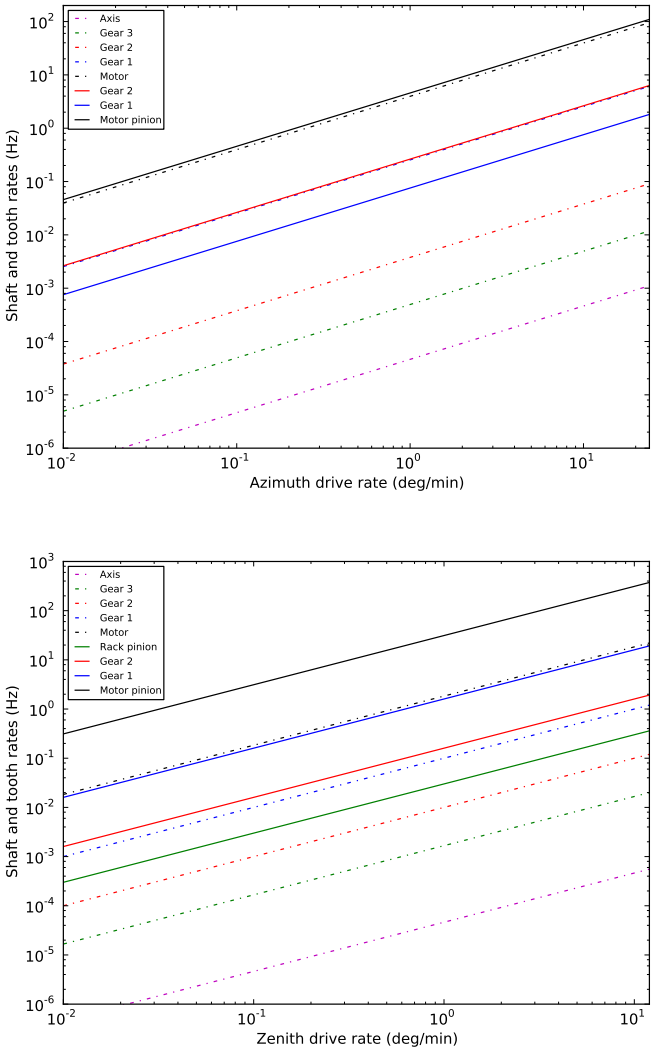

Figure 15: Graphs showing the shaft and tooth frequencies in each drive over the range of driving speeds.

References

[1] J. A. Macinante *A vibration study of the C.S.I.R.O. 210-ft radio telescope*, Division of Applied Physics preprint, APP 47, March 1966

[2] J. A. Macinante, B. Dorien-Brown, J. L. Goldberg, N. H. Clark, R. A. Glazier and K. M. O'Toole *A vibration study of the C.S.I.R.O. 210-ft radio telescope*, Mechanical Engineering Science, Monograph No. 6, December 1967